

HE-PEx: Efficient Machine Learning under Homomorphic Encryption using Pruning, Permutation and Expansion

Ehud Aharoni*, Moran Baruch*, Pradip Bose†, Alper Buyuktosunoglu†, Nir Drucker*, Subhankar Pal†, Tomer Pelleg*, Kanthi Sarpatwar†, Hayim Shaul*, Omri Soceanu*, Roman Vaculin†

†IBM T.J. Watson Research Center, Yorktown Heights, NY, USA *IBM Research - Haifa, Haifa, Israel
Email: subhankar.pal@ibm.com

ABSTRACT

Privacy-preserving neural network (NN) inference solutions have recently gained significant traction with several solutions that provide different latency-bandwidth trade-offs. Of these, many rely on homomorphic encryption (HE), a method of performing computations over encrypted data. However, HE operations even with state-of-the-art schemes are still considerably slow compared to their plaintext counterparts. Pruning the parameters of a NN model is a well-known approach to improving inference latency. However, pruning methods that are useful in the plaintext context may lend nearly negligible improvement in the HE case, as has also been demonstrated in recent work.

In this work, we propose a novel set of pruning methods that reduce the latency and memory requirement, thus bringing the effectiveness of plaintext pruning methods to HE. Crucially, our proposal employs two key techniques, *viz. permutation and expansion* of the packed model weights, that enable pruning significantly more ciphertexts and recuperating most of the accuracy loss, respectively. We demonstrate the advantage of our method on fully connected layers where the weights are packed using a recently proposed packing technique called tile tensors, which allows executing deep NN inference in a non-interactive mode. We evaluate our methods on various autoencoder architectures and demonstrate that for a small mean-square reconstruction loss of 1.5×10^{-5} on MNIST, we reduce the memory requirement and latency of HE-enabled inference by 60%.

KEYWORDS

homomorphic encryption, neural networks, machine learning, pruning, tile tensors, privacy-preserving computation

1 INTRODUCTION

Data privacy and confidentiality are of utmost priority in today's world that is driven by information exchange. Outsourcing sensitive data to a third-party cloud environment, while complying with regulations such as GDPR [17] and HIPAA [14], is the need of the hour for many companies and organizations, such as banks and medical establishments. One promising solution that has been garnering significant traction is the use of homomorphic encryption (HE), which allows for the evaluation of certain functions on encrypted inputs. Gartner corroborates the massive potential of such privacy-preserving techniques, predicting that 50% of large organizations will adopt such computation models for processing in untrusted environments for multi-party data analytics, by 2025 [19]. Corporations and academic organizations have already begun investing resources into developing secure and efficient solutions,

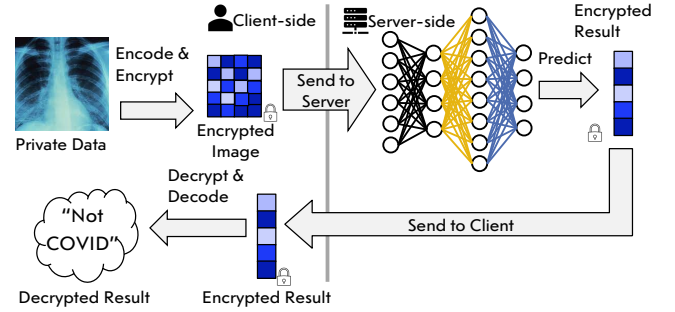


Figure 1: An illustration of a typical two-party (client-server) classification flow for detecting COVID-19 using patients' X-Ray images under HE.

exemplified by the list of companies that are actively participating in initiatives such as HEBench [2] and the HE standardization effort [6]. The major challenge that is constraining faster adoption is that HE applications involving a large number of operations, such as inference on large machine learning (ML) models under HE, is at best a few orders-of-magnitude slower than their plaintext counterparts and has significantly more memory requirements [4].

Privacy-preserving Machine Learning (PPML). We focus on the use of HE in the context of privacy-preserving machine learning (PPML) inference frameworks. These frameworks run on systems that involve at least one client and one server, where the clients desire the privacy of input data (e.g. images), and the server performs inference over an encrypted ML model, which has been trained with proprietary data. Further, we focus on a non-client aided solution model that is illustrated in Figure 1, where the client (a hospital) dispatches encrypted images of the patient's X-Ray images for classification from a server that runs inference under HE without any client interaction. The encrypted result is decoded and decrypted on the client-side to reveal the outcome.

Ciphertext Packing. Typical HE schemes perform computation in the form of single instruction multiple data (SIMD). For instance, in the CKKS scheme [15], $N/2$ input elements are packed into two ciphertext vectors of size N each. In general, multi-dimensional inputs may be packed using different approaches, such as row-wise, column-wise, element-wise, diagonal-wise, where the choice of packing method may dramatically affect the latency and memory of the HE computation. One recent work, called HeLayers [3], is a framework that proposes efficient packing of multi-dimensional inputs by decomposing the input into tiles that are each packed into a separate ciphertext. For example, a simple 25×25 grayscale image may be packed into a set of 49 ($= \lceil \frac{25}{4} \rceil \cdot \lceil \frac{25}{4} \rceil$) 4×4 tiles.

Neural Network (NN) Pruning. The problem of complex and large ML models with high memory and latency requirements is not unique to the domain of PPML, as it also exists in standard ML. One commonly used technique to address this limitation is pruning, *e.g.* pruning neural network (NN) convolutional filters, fully connected (FC) weights or even entire nodes from a trained model [8, 25, 26, 38, 42]. In practice, these methods are used as a form of model compression to reduce model sizes for better resource utilization and performance, while minimizing accuracy loss.

We adapt various NN pruning strategies from plaintext ML to our scenario of non-interactive HE under SIMD packing and show that they fail for any reasonably-sized packing shape. This is due to the fundamental reason that while pruning may introduce zeros, if the zeros reside in a ciphertext where even one other element is a non-zero, then the ciphertext cannot be eliminated. For instance, when we aggressively pruned 85% of weights in our network with our best pruning scheme, only 17% of the ciphertexts were eliminated.

Our Contributions. We propose a framework called **HE-PEX** that builds on a set of four primitives, *viz.* pruning, permuting, packing, and expanding, to achieve superior pruning ratios while maintaining low accuracy loss. While our methods are applicable to convolutional NNs, they best-suited for networks with cascaded FC layers. Thus, we demonstrate our techniques on autoencoders, which generally use these layers.

Our contributions can be summarized as follows:

- We introduce a new set of methods to perform packing-aware pruning, which combines four main primitives: prune, permute, pack, and expand. Specifically, we provide a novel permutation algorithm for NNs that contain sequences of FC layers.
- We integrate this framework with HeLayers [3] to create a holistic toolset that takes in an input model and automatically produces a pruned and packed network that meets various user constraints, such as accuracy, latency and memory requirement.
- We adapt a state-of-the-art pruning technique called Hunter [13] to HeLayers that supports non-interactive HE evaluations of deep NNs, which serves as a baseline for our experimentation.
- We implement and compare several of these schemes on a set of three ML networks for tile tensors with different tile shapes, comparing their accuracies and ciphertext reduction fractions.

Our results show reductions of 85% and 60% in zero tiles for tile sizes of 2×2 and 16×16 , respectively, with an output reconstruction loss of 1.5×10^{-5} . The memory and latency of performing end-to-end inference operations using our largest network resulted in $\sim 60\%$ memory and latency reduction, with the same loss.

Paper Organization. The rest of the paper is organized as follows. Section 2 discusses related work on pruning for PPML. Section 3 describes the notation used in the paper and provides some background about NN pruning, HE, and tile tensor based packing [3]. Section 4 presents details of our framework, including our novel permutation and expansion algorithms. Our experimental setup is discussed in Section 5, and the results of our experiments are reported in Section 6. Finally, we discuss some interesting takeaways in Section 7 and conclude the paper in Section 8.

2 RELATED WORK

A few recent works port NN pruning techniques to the PPML domain. Yang *et al.* [52] propose a new FPGA design that can efficiently handle sparse ciphertexts. It assumes a network that is pruned based on some standard pruning method and leverages the fact that some ciphertexts happen to encrypt zeros. Cai *et al.* propose an improved pruning method called Hunter [13], where the pruning is applied in an HE packing-aware pruning manner. The pruning considers the way the data is encoded and encrypted into the HE ciphertexts, which eventually reduces the number of ciphertexts used for computation and thus reduces the overall latency and memory consumption. The packing-based pruning method of Hunter [13] is demonstrated using the specific packing choice of the client-aided solution GAZELLE [31], where the client evaluates the activation functions. HE-PEX, instead, targets a non-interactive scenario in which the server computes the activation layers and therefore should perform an online sequence of encrypted matrix multiplications. We adapt the Hunter scheme to this scenario (termed: P2T) and compare this against our other techniques. While we focus on non-interactive designs, we argue that HE-PEX is equally valuable for interactive designs.

Chou *et al.* [16] use pruning to reduce the number of weights, and quantization to convert them to powers-of-2, which results in sparse polynomial representations. Their techniques reduce the number of costly multiplication operations and improved the overall latency. While [16] uses pruning in the context of HE, it does not pack the network after pruning to maximize ciphertext density, as we do. Another work [51] considers pruning of convolution layers in the context of Paillier encryption [43], and [45] considers pruning in the context of garbled circuits (GCs), however their algorithm is different from ours and does not consider packing with tile tensors.

NN pruning was also considered by Gong *et al.* [22] in the context of PPML, where the goal was to maintain the privacy of the data in the training dataset. However, neither the model nor the data is encrypted and their privacy aspect lies with the training data, and not the data used during inference or the model weights.

Finally, like Hunter [13], our approaches used in HE-PEX are orthogonal to a line of research on privacy-preserving neural architecture search (NAS) [20, 29, 36, 39] that aim to find more efficient PPML architectures, while considering the underlying cryptographic primitives. For example, because it is hard to perform non-linear operations using HE, such a search can target finding NNs with less non-linear operations compared to a baseline.

3 BACKGROUND

This section provides the reader with some background on HE and a recent method of efficiently packing ciphertexts called tile tensors. We conclude this section with our assumed threat model.

3.1 Homomorphic Encryption

An HE scheme is an encryption scheme that allows us to evaluate any circuit, and in particular any function, on encrypted data [24]. Modern HE instantiations such as BGV [12], B/FV [11, 18], and CKKS [15] rely on the hardness of the Ring-LWE problem, support SIMD operations, and operate over rings of polynomials. HE schemes generally support six methods, *viz.* *Gen*, *Enc*, *Dec*, *Add*, *Mul*

and *Rot*. The function *Gen* generates a secret key public key pair. The function *Enc* receives a message that is a vector M with s elements, and returns a ciphertext. The function *Dec* receives a ciphertext and returns an s -dimensional vector. An HE scheme is correct if for every input vector M , $M = \text{Dec}(\text{Enc}(M))$ and is approximately correct (as in CKKS) if for some small $\epsilon > 0$ that is determined by the key it follows that $|M(i) - \text{Dec}(\text{Enc}(m))(i)| \leq \epsilon$. The functions *Add*, *Mul* and *Rot* are thus defined as follows.

$$\begin{aligned} \text{Dec}(\text{Add}(\text{Enc}(M), \text{Enc}(M'))) &= M + M' \\ \text{Dec}(\text{Mul}(\text{Enc}(M), \text{Enc}(M'))) &= M * M' \\ \text{Dec}(\text{Rot}(\text{Enc}(M), n))(i) &= M((i + n) \bmod s) \end{aligned}$$

3.2 Non-Interactive Homomorphic Encryption

Many frameworks offer PPML inference solutions using HE or a combination of it with multi-party computations (MPC) protocols, such as GCs, oblivious transfers (OTs) or secret sharing (SS) [3, 9, 10, 21, 30, 31, 35, 37, 39–41, 44–47, 49, 50]. Protocols that exclusively use HE, such as [3, 37], are called non-interactive or non-client-aided protocols, while the others are termed interactive or client-aided. In the client-aided approach, the server asks the client for assistance with the computation, *e.g.* to compute a non-polynomial function, such as ReLU, that is not supported natively in HE. Here, the server asks the client to decrypt the intermediate ciphertext data, perform the ReLU computation, and re-encrypt the data using HE. This approach is implemented, for example, in GAZELLE [31] and nGraph-HE [10]. Here, the server utilizes MPC to hide the intermediate results from the client.

The main drawback of client-aided solutions is that the client must stay online during the computation. Moreover, Akavia and Vald [5] demonstrate that this approach may involve some security risks, and Lehmkuhl *et al.* [34] show that it can even make it easier to perform model-extraction attacks. To this end, our focus is on non-client-aided solutions, where the computation is done entirely under encryption, without interaction. However, we stress that our proposed methods are also applicable to interactive solutions.

3.3 Ciphertext Packing using Tile Tensors

HE schemes, which operate on ciphertexts in a SIMD fashion such as BGV [12], B/FV [11, 18], and CKKS [15] allow encrypting a fixed size vector into a single ciphertext, and the homomorphic operations on the ciphertext are performed slot-wise on the elements of the plaintext vector. The use of SIMD also makes it faster to execute on modern processors that support efficient operations on vectors of data. To utilize this, we need to pack and encrypt more than one input element in every ciphertext. The choice of packing method can dramatically affect the *latency* (time taken to perform the computation), *throughput* (number of computations performed within a unit of time), communication costs (*e.g.* server-client bandwidth requirement), and memory requirement.

A recent work by Aharoni *et al.* [3] proposes a data structure called *tile tensor* that packs tensors (*e.g.* vectors, matrices) into fixed-size chunks, called *tiles*. Due to the property of them having fixed sizes, tile tensors are a natural fit for HE, as each tile can be encrypted into a single ciphertext, where each element of the tile is mapped into a separate slot in the ciphertext. The authors

of [3] demonstrate the use of tile tensors to implement various layers of a NN. As an example, they consider encrypted inference on AlexNet [32], which is a classic network for image classification, and improve its execution time over the previous state-of-the-art by several orders-of-magnitude. In their solution, they employ 5-dimensional tiles, which they denote as C, X, Y, F, B , where C is the *channel* dimension encoding the channels of the input, X and Y are the width and height dimensions of the image, F is the *filter* dimension encoding the different filters of each layer, and B is the *batch* dimension encoding the different images to classify.

The authors illustrate that the same tensor can be packed into tiles of different shapes, but of the same size (*i.e.* capacity). For instance, while a matrix may be naïvely packed into column-vectors or row-vectors, it can also be packed into two-dimensional tiles, as long as the tile size matches the number of slots in the ciphertext. In addition, tile tensors allow for other manipulations, such as duplicating elements along one or more dimensions. This is necessary, for instance, when there is a batch dimension to the input and the weights need to be replicated to construct three-dimensional tiles. It is important to note that the security level of the scheme depends on the size of the tile and not on the individual dimensions. The paper shows that different tile shapes lead to different trade-offs. For instance, one tile shape may require more memory but be optimal in terms of execution time, while another shape may be trade-off execution time for a smaller memory footprint. To this end, the framework proposed in [3], called HeLayers, uses an optimizer to navigate the configuration space of tile shapes to find one that optimizes for a given objective function.

In the context of HE-enabled NN pruning, packing the neurons and weights of a NN into tiles raises an important challenge: *efficient pruning can be done only in the resolution of an entire tile* (*i.e.* ciphertext) and not at that of a single neuron or weight. This is the exact problem that HE-PEx sets out to address.

3.4 Threat Model

Our threat model involves three entities: (i) an AI model owner, (ii) a cloud server that performs model inference on HE encrypted data using the pre-computed AI model, and (iii) a user who sends confidential data to the cloud for model inference.

We take into account the following scenarios, among others.

- (1) The users and the model owner belong to the same organization, where both have access to the private key and are allowed to see the encrypted data.
- (2) The model owner is the private-key holder. The user uses the public key to encrypt their samples before uploading them to the cloud. The model owner can decrypt and distribute the inference or post-processed results to the users. This scenario involves a non-collusion assumption between the model owner and the cloud.
- (3) The user is the private-key owner. The model owner can use the public key to encrypt its model before uploading it to the cloud. This scenario involves a non-collusion assumption between the user and the cloud.

In all cases, the cloud should learn nothing about the underlying encrypted data. In (2) and (3), the users should not learn the model,

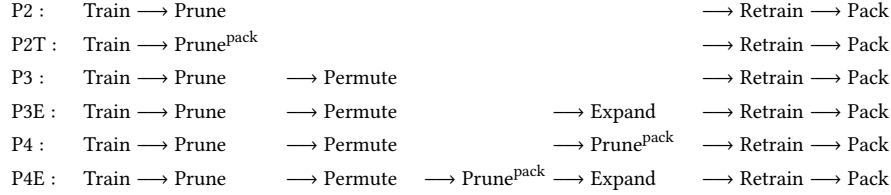


Figure 2: Overview of our prune, permute, expand, and pack methods as part of HE-PEX.

excluding privacy attacks, where the users try to extract the model training data from the inference results.

We assume that communication between all entities are encrypted using a secure network protocol, *i.e.* a protocol that provides confidentiality, integrity, and allows the model owner and the users to authenticate the cloud server, such as TLS 1.3. The model owner can send the model to the server either in encrypted format or in the clear. If the model is encrypted, the server should learn nothing about the model but its structure. In both cases, we assume that the cloud is semi-honest (or honest, but curious), *i.e.* that it evaluates the functions provided by the data owner and users without any deviation. We stress that our proposed methods modify the data arrangement *before* encryption, and thus do not affect the semantic security properties of the underlying HE scheme. Finally, in our experiments we target an HE solution with 128-bit security.

4 HE-PEX FRAMEWORK

We first introduce our framework, called HE-PEX, and explain the pruning methods we incorporate as part of it. We then describe our simple but powerful permutation algorithm that effectively increases the ciphertexts that can be discarded with zero change in inference accuracy. The next part discusses the confidentiality implications of our schemes. We conclude with a description of how we integrate it as part of HeLayers [3].

4.1 Prune, Pack, Permute and Expand Methods

We introduce several methods that we list in Figure 2. Every method starts by training a NN; it could train from scratch or start with a pre-trained model. Once the network is trained, we prune its neurons or weights based on some criterion. While there are plenty of pruning configurations, we consider only a few standard methods that we summarize in Table 1. Note that a better pruning method can only serve to improve our reported results. In the rest of the paper, we denote the various pruning techniques by $\{scope\}/\{criterion\}/\{target\}$.

Universally, our pruning methods accept a pruning fraction as input which indicates the fraction of the target to prune, where the target can be weights or neurons. Weight pruning is illustrated in Figure 3 (i)-(ii). We focus on weight pruning in this work, as pruning neurons can raise the question of whether the pruning technique really helps or if we could have just started with a smaller network, to begin with. This is an interesting philosophical question as many users today consider off-the-shelf NNs such as ResNet-20 [27] or AlexNet [32] when training a new model. In that case, *i.e.* in the common scenario for data scientists, pruning neurons helps. For completeness, we measure and report our results for both targets. We do not consider bias pruning separately.

Table 1: Scope, criterion and target of pruning in each of the variants of HE-PEX.

P2T	Scope	Local (Lc), Global (Gl)
	Criterion	Average/Maximum/Minimum of tile (T-Avg/T-Max/T-Min)
	Target	Weight (-)
P2, P3, P3E	Scope	Local (Lc), Global (Gl)
	Criterion	L1 (L1), Rand (Rnd)
	Target	Weight (Wei), Neuron (Neu)
P4, P4E	Scope	Local (Lc), Global (Gl) [1st and 2nd prune]
	Criterion	L1 (L1), Rand (Rnd) [1st prune], threshold fraction of non-zeros in tile to prune [2nd prune]
	Target	Weight (Wei), Neuron (Neu) [1st prune]

The pruning criteria we consider include (i) pruning uniformly at random, *i.e.* randomly pruning neurons or randomly setting weights to zero, and (ii) pruning based on some threshold, *e.g.* the L1-norm of a weight, or of the set of incoming/outgoing weights of a neuron. We will describe the additional criteria for P2T, P4 and, P4E later.

The scope of pruning indicates whether the pruning is done layer-by-layer, or all at once. When using the random criterion, the scope does not have an effect. However, it has a major effect when considering, *e.g.* L1-based pruning, particularly if there is a large variance in the weights across the different layers. Here, if we prune 50% of the network, it might be the case that only the initial layers are pruned. To summarize, we consider five pruning configurations based on valid combinations of the parameters in Table 1, *viz.* $Lc/L1/Wei$, $Gl/L1/Wei$, $-/Rnd/Wei$, $Lc/L1/Neu$ ¹ and $-/Rnd/Wei$.

All strategies except for P2T first perform pruning by one of the pruning configurations defined above. P2T uses a tile packing-based pruning configuration that is distinct from the above. Here, we first pick a tile shape and split every matrix into tiles, as illustrated in Figure 3 (i) with 2x2 tiles. For every tile, we compute the minimum-/maximum/average metric of its values and prune the tiles with the lowest value of the metric. We refer to these options under the (reduction) criteria in Table 1 and denote this pruning as $prune^{pack}$ in Figure 2. Note that this is our adaptation of Hunter [13] to tile tensors [3], which we compare with other strategies.

Note that only P2T performs packing-based pruning right away, and because it prunes complete tiles, there is no need to perform further steps such as permutation or expansion. The con is that each tile may harbor a wide range of weights, and so important weights may get pruned in this process. In contrast, a non-packing-aware pruning may be more efficient in terms of pruning the “right” weights, however, the pruned weights or neurons are not necessarily organized in a way that is packing-friendly and will lead to a

¹ $Gl/L1/Neu$ was not evaluated since PyTorch limits the scope of global pruning to unstructured methods only.

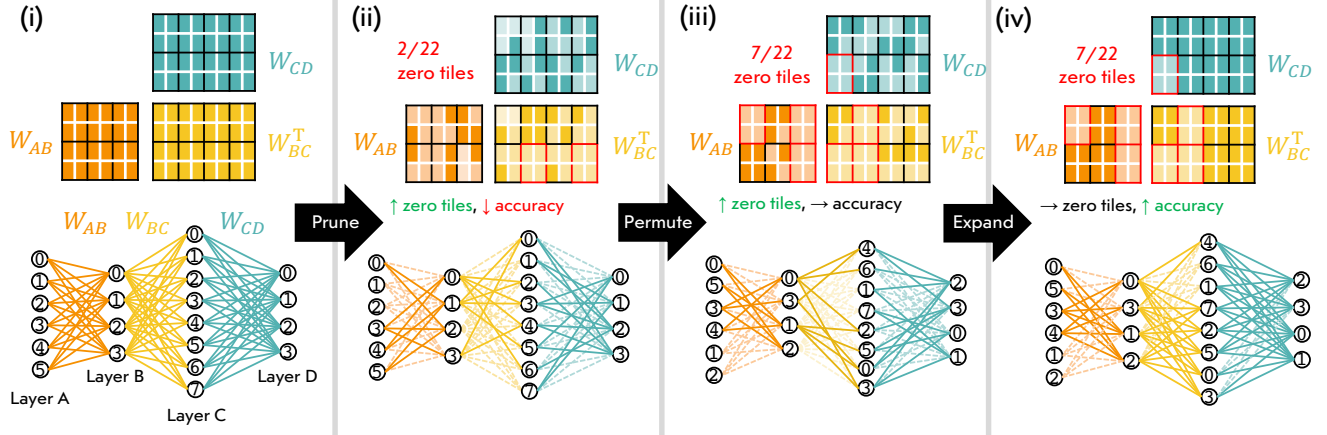


Figure 3: Illustration of our prune-permute strategy for the P3E scheme when considering a 4-layer network with 6,4,8,4 neurons in layers A-D, respectively. We divide the weight matrices into 2×2 tiles and perform $54/88 = 61\%$ weight-based pruning. After pruning we can only reduce $2/22 \approx 10\%$ tiles. After permutation, however, it is possible to reduce $7/22 = 35\%$ of the tiles. Expansion (with an implicit post-expansion re-training step) is useful to restore most of the accuracy loss.

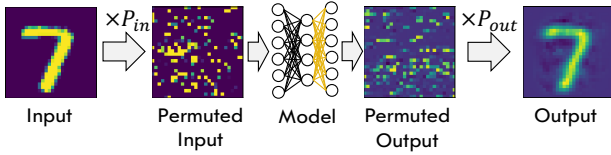


Figure 4: Illustration of the two additional operations required for inference on a permuted autoencoder network. These are performed on the plaintext input and output.

wide cancellation of tile operations. Therefore, we propose to apply additional steps that we describe next.

The permute and expand operations are illustrated in Figure 3 (ii)-(iv). The *permute* operation permutes the rows and columns of the weight matrices after the pruning operation to essentially congregate the zero elements together. The detailed algorithm that we deploy is described in Section 4.2. The *expand* operation is a reversal of the pruning operation, where we search for tiles that are *not completely zero*, i.e. they hold zeros and non-zeros, and we un-prune the zero elements inside them. The motivation behind this action lies in the motivation to perform pruning, which is to reduce the number of active tiles. If a tile is not reduced, i.e. it has non-zero elements, then we cannot ignore it, and because we do not gain any performance benefits, it is best to fully utilize its elements to improve the accuracy of the model.

The strategies described above form the foundations of the schemes P2, P2T, P3, and P3E, as shown in Figure 2. To complete the set, we construct two more strategies, called P4 and P4E. In P4, instead of expanding the model as in P3E, we perform a second pruning-aware-packing step to reduce tiles that contain “mostly” zeros. These tiles are selected based on whether the tile has more than a certain fraction of non-zeros, which is an additional criterion for this scheme (see Table 1). Lastly, we note that we experimented with two more schemes, where after the first permutation step, we perform a semi-packing-aware-pruning method that locates mostly-zero tiles and prunes a few elements inside them (but not

all). Subsequently, we reapply the permutation algorithm, with the idea being to help the permutation heuristic while sticking with the pruning configuration that was originally applied. After the second permutation, we either expand or packing-aware-prune tiles based on the number of zeros inside them. These schemes led to unstable behavior with regard to the loss function in our experiments, and thus we do not discuss these further in the rest of the paper.

4.2 Permutation Algorithm

We illustrate here an efficient way of increasing the number of zero tiles given a pruned network and a tile tensor shape. We first describe the algorithm for the case of a single weight matrix (an FC layer) and then extend the idea to multi-layered NNs. We note that in addition to a permuted network, our algorithm produces two permutation matrices, P_{in} and P_{out} , which are multiplied with the input and output, respectively, at the user’s end. Since these are just two plaintext operations, the overhead for this is negligible compared to the HE computation.

One naïve way to obtain the matrix with the greatest number of zero-tiles is an exhaustive search. However, this method has a complexity of $O(M!N!)$ for an $M \times N$ weight matrix, which quickly gets prohibitive as the size of the layer increases. To make this problem tractable, we instead propose to permute the rows and columns based on iterative clustering algorithms. Specifically, we illustrate our proposal using the well-known k -means clustering technique, which we show in Figure 5. We note that we use a balanced version of k -means, as we require the size of each cluster to exactly match the tile shape. However, our idea is not restricted to k -means and is equally compatible with other clustering techniques, such as agglomerative clustering [23] and graph partitioning techniques such as Ncut [48]. The rows of the pruned weight matrix are considered as vectors and k -means is applied to produce a new weight matrix with the rows permuted to increase the number of zero-tiles. Then this matrix is transposed, and the process is repeated till convergence. Here, the distance function used is Hamming distance with

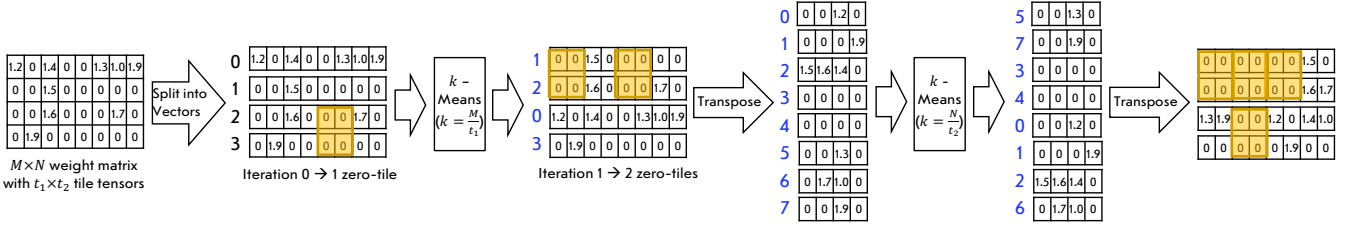


Figure 5: Permutation of a single $M \times N$ weight matrix considering tile tensors with the shape of $t_1 \times t_2$, with zero tiles highlighted. Permutation is able to efficiently rearrange the weights without affecting the outcome of operations that use the weights. In this example, two k -means iterations are sufficient to reach the permutation with the maximum number of zero tiles.

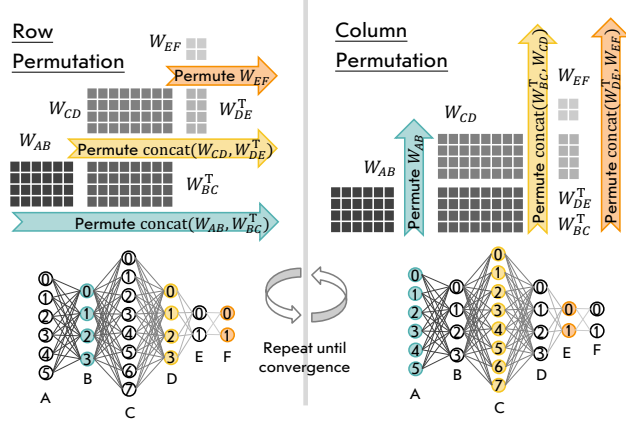


Figure 6: An illustration of weight permutation in a multi-layered network. The permute operations correspond to permuting the highlighted neurons.

the non-zero cells being treated as a 1. The number of clusters for k -means is equal to the number of tiles along the rows or columns, depending on the iteration being performed.

Multi-Layer Permutation. In the case of a single weight matrix (an independent FC layer), one can permute the rows and columns independently. For a deeper network, however, the weights for adjacent layers are also affected when permuting the rows/columns of a given layer. Consider the network in Figure 6. Shuffling the neurons in layer B translates to permuting the rows of the weight matrix W_{BC}^T , however this also permutes the rows of the preceding weight matrix W_{AB} . Thus we need to permute the rows of W_{AB} and W_{BC}^T in tandem (treating them as a concatenated matrix), and similarly for W_{CD} and W_{DE}^T in the case of permutations of neurons in layer D, and W_{EF} for layer F. In the next iteration, we permute the columns of the remaining sets of weights, which corresponds to permuting the neurons in layers A, C and E. This process is repeated till convergence. As is evident, this technique essentially discovers a re-arranged network such that the packing method can discard the maximum number of ciphertexts (tiles) that contain only zeros, thus benefitting both memory and latency, and without affecting the model (and thus accuracy).

4.3 Integration with HeLayers

As alluded to previously, we integrate HE-PEx with HeLayers [3] and Figure 7 shows the flowchart of our P4E strategy. This flowchart

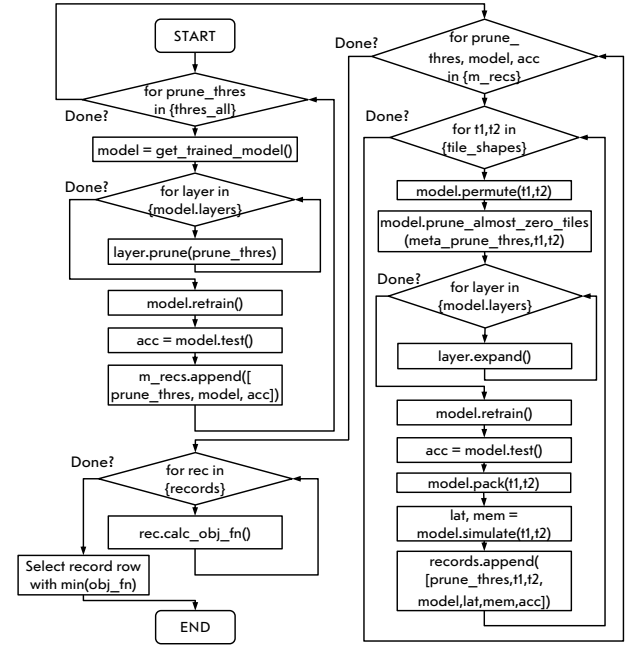


Figure 7: Flowchart illustrating the P4E strategy with local pruning scope for the prune step and global scope for `prunePack`. This is executed as a pre-deployment step on the entity that has access to the plaintext network parameters.

can be extended as needed to the other strategies discussed in Section 4.1. We illustrate a grid-search approach in this flowchart with $\{thres_all\}$ and $\{tile_shapes\}$ being a pre-selected set of values ($meta_prune_thres$ may be constant or swept) and the output of the framework is a model ready for deployment that meets an objective function based on latency, accuracy and/or memory requirement. A local-search strategy can similarly be considered to navigate the exploration state space with fewer training and permutation rounds, which are the most time-consuming segments of this flow.

4.4 Security Analysis

The confidentiality of the model or the user data is agnostic to the use of HE-PEx, because the pruning phase happens in plaintext before uploading any data to the server. Once the data is encrypted its security relies on the semantic security of the underlying HE algorithm, such as BGV [12], B/FV [11, 18], or CKKS [15], which

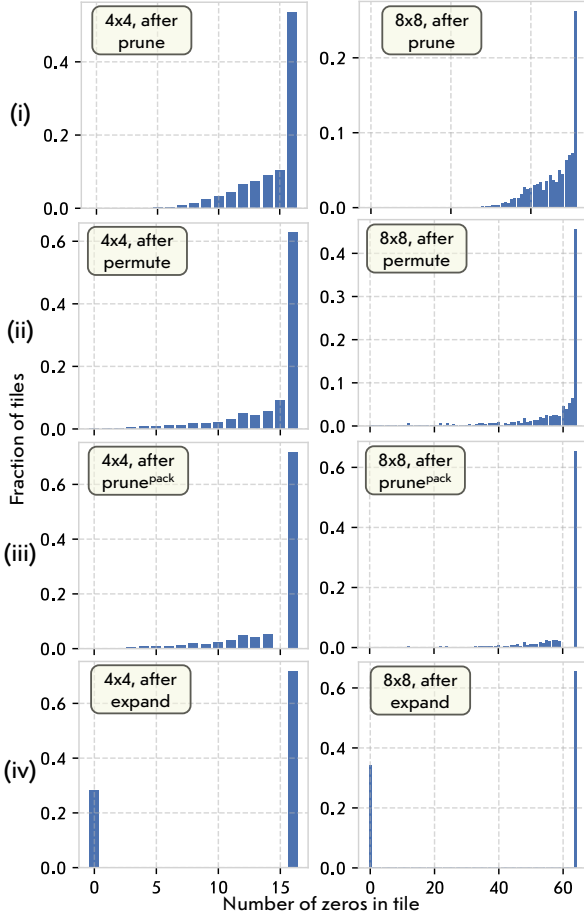


Figure 8: Histograms of zero elements in 4×4 and 8×8 tiles, after performing Lc/L1/Wei pruning of 90% of the weights in Autoenc₂, before and after applying our permutation and extension algorithms (P4E scheme). The x-axis is the number of zeros in tile and the y-axis is the fraction of tiles.

means that the server can perform any operation on the ciphertexts without revealing the underlying plaintexts. Another advantage of using a non-interactive design is that it relies only on the HE primitive and does not rely on other cryptographic primitives such as GCs, OT, or SS. Note that by pruning a model we only reduce the amount of computation that a server needs to perform and we do not introduce new computation mechanisms.

The use of pruning can raise the following concerns: can the structure of the model leak information? That is, can an adversary learn something about the training or test data based solely on the reduced architecture? Can an adversary learn something if it knows the original structure and can observe the new structure? This concern applies to our work as well as prior work such as [13]. We are unaware of previous reports on such attacks and we see it as an interesting research question. Consequently, this paper assumes that no meaningful leakage happens from using a reduced model, except for the final model architecture, which includes the position of the zero tiles and is always visible when using HE. Lastly, as stated in Section 1, we leave outside the scope of this paper attacks such

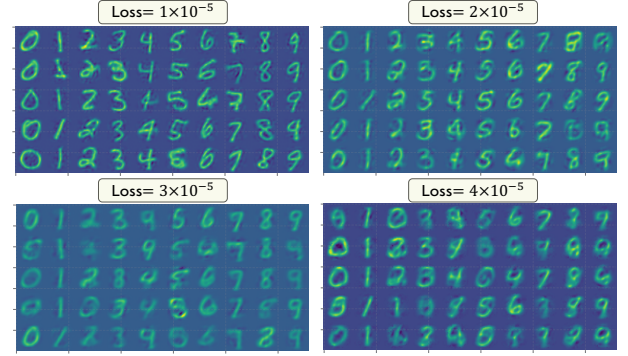


Figure 9: Visualization of the autoencoder output reconstructed image for different loss values using MNIST.

as model-extraction, model-inversion and inference-membership attacks that can result from treating the model as a black-box.

5 EXPERIMENTAL SETUP

Our experiments involving the methods in Section 4.1 are done on a cluster of server-class machines, each equipped with two NVIDIA® Tesla® V100 SXM2 GPUs with an Intel® Xeon® Gold 6258R CPU @ 2.70GHz. We used PyTorch version 1.11.0 accelerated with CUDA 11.6. For end-to-end evaluation using HeLayers [3], we used an Intel® Xeon® CPU E5-2699 v4 @ 2.20GHz machine with 750GB memory and 44 cores. We observed that for our pruned networks, not all of the cores were fully utilized and performance saturated around 8 cores. Thus, for a fair comparison, we limited the system to use 8 cores for all of our experiments. We use HeLayers [3, 28] with the CKKS SEAL [1] implementation targeting 128-bit security, and the reported results are the average of 10 runs.

Dataset and Network Architectures. Our experiments involve three vanilla autoencoder network architectures, in which every FC layer is followed by an activation layer. We use square activations instead of typical ReLU activations to support non-interactive solutions that require HE-friendly networks.

- Autoenc₁: a network with 1 FC layer of size 32.
- Autoenc₂: a network with 1 FC layer of size 64.
- Autoenc₃: a network with 3 FC layers of sizes 64, 32, and 64.

We trained the networks on the MNIST dataset [33], which contains 60,000 images of $28 \times 28 \times 1 = 784$ pixels. Consequently, the autoencoder’s input size is 784, as is its output size. We train the encoder and decoder parts of the network together in our experiments. We stress that our methods are by no means restricted to autoencoders; these are simply used as a vehicle for our evaluation.

Training Parameters. The number of {training epochs, re-training epochs} for Autoenc₁, Autoenc₂, Autoenc₃ were set to {20, 10}, {30, 20}, and {30, 20}, respectively. We use batches of ten samples for training and set the learning rate of the Adam optimizer to 0.001. Following previous work on autoencoders, we set our loss function to be the mean-square error (MSE) between the input image and the output (reconstructed) image, and use the same as a proxy for the performance (accuracy) of the model. A visualization of the raw loss values is shown in Figure 9.

Tile Shapes. Without loss of generality, we perform our experiments with tile tensors of dimensions $[t_1, t_2, t_3]$, where $t_1 = t_2$

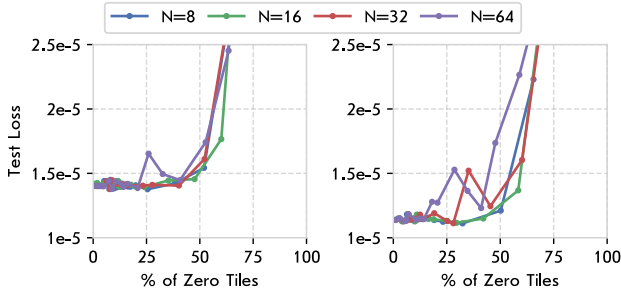


Figure 10: Test loss (y-axis) and percentage of zero tiles (x-axis) with a tile shape of 16×16 for our P4E scheme (Autoenc₂: left and Autoenc₃: right) with different values of N , where N is the threshold of non-zeros per tile equal to or below which the entire tile is pruned ($Lc/Ll/Wei$).

corresponds to the width and height of tiles in the weight matrices, and t_3 is the size of the batch. Specifically, we set t_1 to be $2/4/8/16$ and adapt t_3 so that the final tile (ciphertext) size in all cases is the same, e.g. setting $t_1 = t_2 = 16$ with a batch size of 64 results in the same tile size as with $t_1 = t_2 = 4$ and a batch size of 1,024.

Enhancing HeLayers. HeLayers [3] uses data structures called `CtileTensor` and `PtileTensor` to hold tile tensors of encrypted and unencrypted data, respectively. These use an API called `encode` to encode or pack the data before encrypting it. We enhance HeLayers to automatically identify zero tiles by modifying the different encoding functions to iterate over each tile and check whether all of its elements are zeros or not. In case a tile contains only zeros, we do not allocate it and instead generate a “zero-flag” to indicate that this is a zero tile. Considering binary addition and multiplication operations that receive two inputs, if only one of the operands has a set zero-flag, then the addition function returns the other operand and the multiplication function returns a `null` tile with the zero-flag set. In the case where both operands are zeros, a `null` tile is returned.

6 EVALUATION

We use this section to first present an in-depth analysis of the P4E scheme, which gave us the best overall results. We then compare P4E with the other methods presented in Section 4.1. Next, we show the performance of the different pruning techniques that have different scopes, criteria and targets. Finally, we present results of running HeLayers on our largest network with the enhancements presented in Section 5.

6.1 Analysis of P4E

To give the reader an intuitive understanding of the impact of each of the critical steps in P4E (Figure 2), we show histograms of the fraction of tiles that have certain number of zeros in them for the Autoenc₂ network with the $Lc/Ll/Wei$ pruning strategy. Prior to the prune step, obviously, most if not all of the tiles have no zeros in them. After pruning 90% of the weights as part of the prune step, only 54% of the tiles have *all* zeros for the 4×4 tile shape. This scenario is even worse for the 8×8 case, where just 26% of the tiles are completely zeros. To explain it, let us assume for simplicity that the weight tensor has a uniform distribution with a density

of p , i.e. each cell is 0 with a probability p . Then, the probability to have a tile of size $m \times n$ with all zeros is p^{mn} , which is reduced when we increase the tile size. In practice, we do not have a uniform distribution because of the locality of large and small weights, and this can be observed in the distributions in Figure 8 (i), which are far from Normal. When the permute step is applied, the weight tensors are rearranged so that more zeros are clustered together, thus increasing the zero-tile percentage to 63% and 46% for the 4×4 and 8×8 case, respectively (Figure 8 (ii)). We thus see a major improvement with permutation, especially for larger tiles.

As we see from the histograms, there are still many tiles that have close-to maximum zeros but that are not exactly zero tiles. The next step in P4E is to carefully prune these *entire* tiles (`prunepack`) such that we can convert them to zero tiles while not penalizing the model accuracy too much. In Figure 10, we illustrate how we pick the pruning threshold (N) for `prunepack` with the example of the 16×16 tile shape. Pruning with $N=16$, i.e. deleting all tiles with less than or equal to 16 non-zeros (6.25% of the tile size), leads to the best overall pruning efficiency without destabilizing the network. Larger values of N cause degradation in model accuracy, as exemplified by their zig-zag behavior in Figure 10, and are thus not considered. The histogram view of the outcome of `prunepack` is shown in Figure 8 (iii).

The final step in P4E (Figure 8 (iv)) is to expand the tiles that have any non-zero left in them. Specifically, expansion refers to re-enabling the cells corresponding to these tiles in the pruning mask of the corresponding weight tensor, which is subsequently followed by re-training to make these cells contain “useful” weights. Although the final model has 72% and 65% zero tiles (corresponding to tile shapes of 4×4 and 8×8 , respectively) given that we started with pruning 90% of the weights, the careful pruning techniques employed in P4E result in a network that still maintains good accuracy, as we will see in the next section.

6.2 Analysis of Pruning Schemes

We now compare a subset of our methods discussed in Section 4.1 – P2, P3, P3E, and P4E, for each of the pruning schemes selected from a combination of scope, criterion, and target (Table 1). These schemes are compared in Figure 11 for four tile shapes, on the basis of test loss and zero tile percentage. Ideally, we would like to pick a scheme that maximizes the zero tile percentage for minimum loss.

We present our analysis in the order of the worst to the best pruning scheme. $-Rnd/Wei$ with P2, which randomly prunes weights in the network, is oblivious to the importance (i.e. value) of the weights and thus affects the accuracy of the network even for conservative amounts of pruning. Moreover, this pruning scheme fails to even get good zero tile fractions as the tile size grows; the fraction of zero tile scales as p^{mn} for a weight pruning fraction of p and $m \times n$ tiles, as mentioned in Section 6.1. Permute (for P3 and P3E) helps, but not by much, as the distribution after permutation is also uniformly random. With expansion, particularly for larger tile sizes, there are hardly any zero tiles left, again owing to the uniform distribution of zeros. P4E, with the combination of two pruning rounds with permutation and expansion, performs the best, but as we will see, other pruning schemes outperform random pruning.

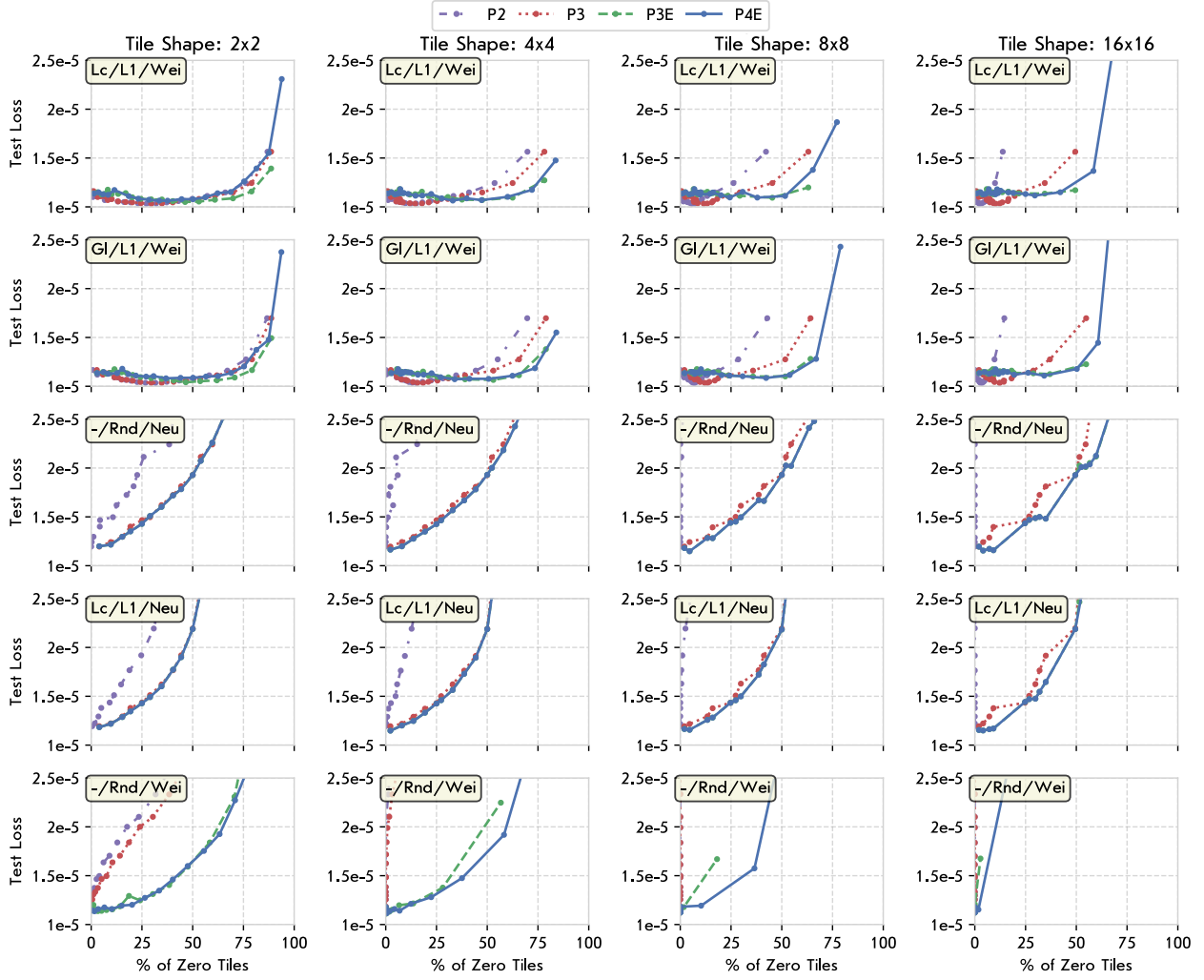


Figure 11: A comparison of our different methods on tiles of size 2×2 , 4×4 , 8×8 and 16×16 (left to right) on Autoenc₂. The y-axis is the value of the mean square error loss function and the x-axis is the percentage of pruned zero tiles. The schemes are ranked from best to worst going downward.

The neuron pruning schemes, $\{Lc/L1/Neu\}$ and $\{-/Rnd/Neu\}$ more graceful degradation of accuracy with pruning and consequently a better trade-off with the percentage of zero tiles. Once permutation is done, the network becomes almost fully-dense, *i.e.* except for the tiles at the right or bottom edge of the weight tensor, which are taken care of by expansion. As a result, P3 performs closely with P3E and P4E, which are exactly equal for these two scenarios.

The local and global L1-norm based weight pruning schemes, $Lc/L1/Wei$ and $Gl/L1/Wei$ give us the best overall trade-off of model accuracy and zero tile fraction. The results considering local pruning scope are slightly better than the global scope for this network (Autoenc₂), however our other experiments show that local performs far better for deeper networks such as Autoenc₃ (not shown in figure). Except for the 2×2 case, P3E and P4E dominate over the other methods. P3E provides networks with losses that are within a small percentage of the original unpruned network. However, the zero tile percentage falls with an increase in tile shape, settling to around 50% for 16×16 tiles (with pruning of 95% of the weights).

P4E is able to push the envelope some more and leads to more zero tiles for some increase in loss. Interestingly, small amounts of pruning under P3 leads to better accuracy than the unpruned network (indicated by the bulges at the base of the curves), as the resultant model generalizes better.

6.3 Comparison with P2T Strategies

We compare our P4E method with our adaption of the scheme by Cai *et al.* [13] to a non-interactive solution, which we refer to as P2T. We construct four variants of P2T, *viz.* $Gl/T-Avg/-$, $Gl/T-Max/-$, $Lc/T-Avg/-$ and $Lc/T-Max/-$. All of these use packing-aware pruning as the first step, with the scope and reduction criterion specified by the first two parameters in the scheme name (Section 4.1).

The results are shown in Figure 12 for each of the three networks and our chosen tile shapes. The local pruning schemes for P2T generally outperform the global scheme, as is true of P4E from Section 6.2. Clearly, P2T is mostly superior for a small tile size

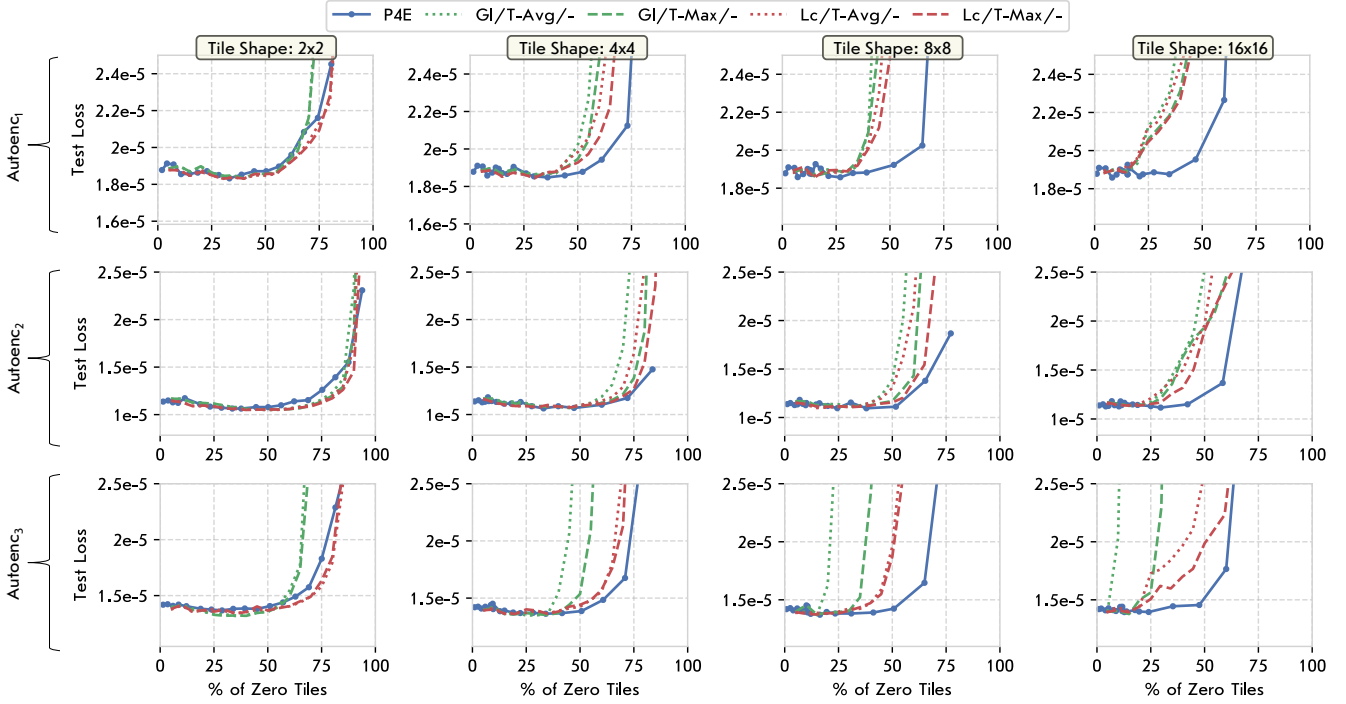


Figure 12: A comparison of the best overall pruning method (P4E, GI/L1/Wei) against P2T variants over different encoders (Autoenc₁, Autoenc₂, Autoenc₃ and different tile sizes (2×2 , 4×4 , 8×8 , 16×16). The y-axis is the value of the mean square error loss function and the x-axis is the percentage of pruned zero tiles.

(2×2 , here), however this scheme quickly degrades as the tile size increases. This is because the variance of weights held in each tile grows with the size of the tile, *i.e.* the larger the tile size, the more the chances that it holds a set of weights that are different in magnitude. When all of these weights are pruned at once, as is done in P2T, it leads to degradation in model accuracy, since important weights are pruned away along with unimportant ones. This is exactly shown by the figures corresponding to tile shapes of 4×4 , 8×8 and 16×16 ; the general trend is that the degradation for P2T is much worse as the tile size increases, compared to P4E. These results effectively showcase the benefits of our prune, permute and expand approaches, in lieu of blind packing-aware pruning schemes, such as P2T.

6.4 Impact on Latency and Memory

Figure 13 shows the latency and memory reduction when running HE-enabled inference on Autoenc₃, considering different percentage of zero tiles across different tile sizes ($t_1 = t_2 = 2/4/8/16$). For the comparison, we fixed the ciphertext polynomial degree to 32,768, which allows it to hold 16,384 values. We also fixed the batch dimension t_3 to 4,096/1,024/256/64 for $t_1 = 2/4/8/16$, respectively. Our results show memory and latency reductions of up to 65% percent when using 2×2 tiles and up to 40% reduction for 16×16 tiles. Table 2 shows a breakdown of the number of HE operations before and after pruning the network. As expected, pruning reduces $\sim 93\%$ of the HE additions and HE multiplications for the case of

Table 2: Number of HE operations when performing an inference operation over Autoenc₃ before and after pruning (*pr*) 95% of the weights for tile sizes of 2×2 and 16×16 .

HE Operation	2×2	2×2 <i>pr</i> (↓)	16×16	16×16 <i>pr</i> (↓)
Addition	24,352	1,693 (93%)	624	231 (63%)
Multiplication	23,869	1,412 (94%)	384	103 (73%)
Rotation	483	281 (42%)	240	128 (47%)
Relinearization	467	265 (43%)	58	30 (48%)

$t_1 = 2$. It also reduces 63% and 73% of the HE additions and HE multiplications, respectively, for the $t_1 = 16$ case.

In both cases, we observe around a 43% reduction in the number of rotations and relinearizations. One explanation is that when using tile tensors for performing matrix multiplication, even with pruning, we still need to execute the rotate-and-sum algorithm to get the final results. In addition, for performance reasons, HeLayers tries to minimize the number of relinearizations by grouping several multiplications together before executing one relinearization.

Table 2 provides an explanation for why there is a potential 30% latency to reduce, even after 95% pruning. Another explanation is that we reduce almost all of the multiplications that are part of the matrix multiplication operations of the network, however, the *output* of each FC layer is likely to not include zero tiles. Therefore, we still have to perform the square activations, which involves multiplication and relinearization operations.

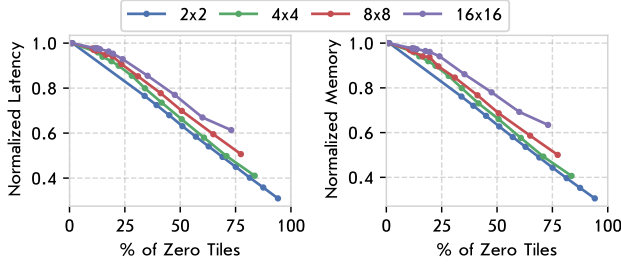


Figure 13: Latency and memory usage when considering different percentage of zero tiles for different tile sizes ($t_1 = t_2 = 2/4/8/16$) when running Autoenc₃ with HeLayers.

7 DISCUSSION

Supporting non-FC Layers. This work demonstrated HE-PEx for networks with FC and activation layers to showcase a focused set of experiments and analyses. However, this does not imply that our methods are not applicable to other layers, such as convolutional layers. Particularly, we did not evaluate HE-PEx with convolutional layers because the fact that convolution filters are generally small, it becomes less interesting to do pruning, permutation and expansion on them. However, HeLayers [3] uses a different convolutional packing method than GAZELLE [31]. It would be interesting to compare the effect of pruning convolutional NNs using our proposed approaches and comparing with other work such as Hunter [13]. We leave this effort for a future work.

Use of other Activation Functions. When using non-interactive designs, we need to substitute typical ReLU activations with HE-friendly activations. For simplicity, we chose to construct our networks using square activations. However, it is possible to use finer-grained approximations, such as higher-degree polynomial-based activations, or trainable activations, to achieve better results [7]. Our methods are orthogonal to the choice of activation function.

Tackling Drawbacks of Non-Interactive Solutions. A common claim in favor of client-aided solutions over non-client-aided ones is that they do not require training a new network, *i.e.* the data model can use an off-the-shelf network, even if it includes non-linear operations that can be executed securely by the client. Clearly, this claim no longer holds when considering client-aided solutions such as Hunter [13], as the model owner needs to prune and retrain the network. In that sense, the cost of also considering HE-friendly layers, *i.e.* only linear operations, becomes negligible, which gets the community one step ahead toward having usable non-interactive HE-based solutions.

8 CONCLUSION

This work presented HE-PEx, a framework of packing-aware pruning for HE-enabled NNs that combines four critical primitives, *viz.* pruning, permutation, expansion and packing. Specifically, we introduce a novel permutation algorithm that rearranges the weights of the network to improve the efficiency of pruning, without affecting the network accuracy. We described how HE-PEx operates in a non-client-aided HE-enabled inference use-case, and integrated it with a general HE packing framework called HeLayers [3] that uses tile tensors for encoding the inputs into ciphertexts. The integrated

framework takes the unpruned network and produces a pruned network along with the tile shape to use for optimally meeting an objective function composed of inference accuracy, latency and memory requirement.

We demonstrated our pruning techniques with various schemes on a set of three HE-friendly autoencoder networks. We adapted a state-of-the-art pruning technique called Hunter [13] to the non-interactive scenario and compared our best scheme against theirs, in terms of reconstruction loss and the fractions of ciphertexts eliminated. Our results with running MNIST on a set of autoencoders showed around a 85% reduction in zero tiles for tile sizes of 2×2 and 60% for larger tiles of size 16×16, under a small reconstruction of 1.5×10^{-5} . Using our techniques for end-to-end inference on our largest network, we observed reductions of 60% for both memory and latency, under the same loss.

REFERENCES

- [1] 2020. Microsoft SEAL (release 3.5). <https://github.com/Microsoft/SEAL> Microsoft Research, Redmond, WA..
- [2] 2022. HEBench. <https://hebench.github.io/>
- [3] Ehud Aharoni, Allon Adir, Moran Baruch, Nir Drucker, Gilad Ezov, Ariel Farkash, Lev Greenberg, Ramy Masalha, Guy Moshkovich, Dov Murik, Hayim Shaul, and Omri Soceanu. 2020. HeLayers: A Tile Tensors Framework for Large Neural Networks on Encrypted Data. *CoRR abs/2011.0* (2020). <https://arxiv.org/abs/2011.01805>
- [4] E. Aharoni, N. Drucker, G. Ezov, H. Shaul, and O. Soceanu. 5555. Complex Encoded Tile Tensors: Accelerating Encrypted Analytics. *IEEE Security & Privacy* 01 (jun 5555), 2–10. <https://doi.org/10.1109/MSEC.2022.3181689>
- [5] Adi Akavia and Margarita Vald. 2021. On the Privacy of Protocols based on CPA-Secure Homomorphic Encryption. *IACR Cryptol. ePrint Arch.* 2021 (2021), 803. <https://eprint.iacr.org/2021/803>
- [6] Martin Albrecht, Melissa Chase, Hao Chen, Jintai Ding, Shafi Goldwasser, Sergey Gorbunov, Shai Halevi, Jeffrey Hoffstein, Kim Laine, Kristin Lauter, Satya Lokam, Daniele Micciancio, Dustin Moody, Travis Morrison, Amit Sahai, and Vinod Vaikuntanathan. 2018. *Homomorphic Encryption Security Standard*. Technical Report. HomomorphicEncryption.org, Toronto, Canada.
- [7] Moran Baruch, Nir Drucker, Lev Greenberg, and Guy Moshkovich. 2022. A methodology for training homomorphic encryption friendly neural networks. In *Applied Cryptography and Network Security Workshops*. Springer International Publishing, Cham.
- [8] Davis Blalock, Jose Javier Gonzalez Ortiz, Jonathan Frankle, and John Guttag. 2020. What is the State of Neural Network Pruning?. In *Proceedings of Machine Learning and Systems*, I. Dhillon, D. Papailiopoulos, and V. Sze (Eds.), Vol. 2. 129–146. <https://proceedings.mlsys.org/paper/2020/file/d2ddea18f00665ce8623e36bd4e3c7c5-Paper.pdf>
- [9] Fabian Boemer, Rosario Cammarota, Daniel Demmler, Thomas Schneider, and Hossein Yalame. 2020. MP2ML: A Mixed-Protocol Machine Learning Framework for Private Inference. In *Proceedings of the 2020 Workshop on Privacy-Preserving Machine Learning in Practice (PPMLP’20)*. Association for Computing Machinery, New York, NY, USA, 43–45. <https://doi.org/10.1145/3411501.3419425>
- [10] Fabian Boemer, Anamaria Costache, Rosario Cammarota, and Casimir Wierzynski. 2019. NGraph-HE2: A High-Throughput Framework for Neural Network Inference on Encrypted Data. In *Proceedings of the 7th ACM Workshop on Encrypted Computing & Applied Homomorphic Cryptography (WAHC’19)*. Association for Computing Machinery, New York, NY, USA, 45–56. <https://doi.org/10.1145/3338469.3358944>
- [11] Zvika Brakerski. 2012. Fully Homomorphic Encryption without Modulus Switching from Classical GapSVP. In *Advances in Cryptology – CRYPTO 2012*, Reihaneh Safavi-Naini and Ran Canetti (Eds.), Vol. 7417 LNCS. Springer Berlin Heidelberg, Berlin, Heidelberg, 868–886. https://doi.org/10.1007/978-3-642-32009-5_50
- [12] Zvika Brakerski, Craig Gentry, and Vinod Vaikuntanathan. 2014. (Leveled) Fully Homomorphic Encryption without Bootstrapping. *ACM Transactions on Computation Theory* 6, 3 (jul 2014). <https://doi.org/10.1145/2633600>
- [13] Yifei Cai, Qiao Zhang, Rui Ning, Chunsheng Xin, and Hongyi Wu. 2022. Hunter: HE-Friendly Structured Pruning for Efficient Privacy-Preserving Deep Learning. In *Proceedings of the 2022 ACM on Asia Conference on Computer and Communications Security (Nagasaki, Japan) (ASIA CCS ’22)*. Association for Computing Machinery, New York, NY, USA, 931–945. <https://doi.org/10.1145/3488932.3517401>
- [14] Centers for Medicare & Medicaid Services. 1996. The Health Insurance Portability and Accountability Act of 1996 (HIPAA). <https://www.hhs.gov/hipaa/>

- [15] Jung Cheon, Andrey Kim, Miran Kim, and Yongsoo Song. 2017. Homomorphic Encryption for Arithmetic of Approximate Numbers. In *Proceedings of Advances in Cryptology - ASIACRYPT 2017*. Springer Cham, 409–437. https://doi.org/10.1007/978-3-319-70694-8_15
- [16] Edward Chou, Josh Beal, Daniel Levy, Serena Yeung, Albert Haque, and Li Fei-Fei. 2018. Faster CryptoNets: Leveraging Sparsity for Real-World Encrypted Inference. *abs/1811.09953* (2018). <http://arxiv.org/abs/1811.09953>
- [17] EU General Data Protection Regulation. 2016. Regulation (EU) 2016/679 of the European Parliament and of the Council of 27 April 2016 on the protection of natural persons with regard to the processing of personal data and on the free movement of such data, and repealing Directive 95/46/EC (General Data Protection Regulation). *Official Journal of the European Union* 119 (2016). <http://data.europa.eu/eli/reg/2016/679/oj>
- [18] Junfeng Fan and Frederik Vercauteren. 2012. Somewhat Practical Fully Homomorphic Encryption. *Proceedings of the 15th international conference on Practice and Theory in Public Key Cryptography* (2012), 1–16. <https://eprint.iacr.org/2012/144>
- [19] Gartner. 2021. *Gartner Identifies Top Security and Risk Management Trends for 2021*. Technical Report. <https://www.gartner.com/en/newsroom/press-releases/2021-03-23-gartner-identifies-top-security-and-risk-management-t>
- [20] Zahra Ghodsi, Akshaj Kumar Veldanda, Brandon Reagen, and Siddharth Garg. 2020. CryptoNAS: Private Inference on a ReLU Budget. In *Advances in Neural Information Processing Systems*, H. Larochelle, M. Ranzato, R. Hadsell, M.F. Balcan, and H. Lin (Eds.), Vol. 33. Curran Associates, Inc., 16961–16971. <https://proceedings.neurips.cc/paper/2020/file/c519d47c329c79537fbb2b6f1c551ff0-Paper.pdf>
- [21] Ran Gilad-Bachrach, Nathan Dowlin, Kim Laine, Kristin Lauter, Michael Naehrig, and John Wernsing. 2016. Cryptonets: Applying neural networks to encrypted data with high throughput and accuracy. In *International Conference on Machine Learning*, 201–210. <http://proceedings.mlr.press/v48/gilad-bachrach16.pdf>
- [22] Yifan Gong, Zheng Zhan, Zhengang Li, Wei Niu, Xiaolong Ma, Wenhao Wang, Bin Ren, Caiwen Ding, Xue Lin, Xiaolin Xu, and Yanzhi Wang. 2020. A Privacy-Preserving-Oriented DNN Pruning and Mobile Acceleration Framework. In *Proceedings of the 2020 on Great Lakes Symposium on VLSI (Virtual Event, China) (GLSVLSI '20)*. Association for Computing Machinery, New York, NY, USA, 119–124. <https://doi.org/10.1145/3386263.3407650>
- [23] K Chidananda Gowda and G Krishna. 1978. Agglomerative clustering using the concept of mutual nearest neighbourhood. *Pattern recognition* 10, 2 (1978), 105–112.
- [24] Shai Halevi. 2017. Homomorphic Encryption. In *Tutorials on the Foundations of Cryptography: Dedicated to Oded Goldreich, Yehuda Lindell* (Ed.). Springer International Publishing, Cham, 219–276. https://doi.org/10.1007/978-3-319-57048-8_5
- [25] Song Han, Huizi Mao, and William J. Dally. 2015. Deep Compression: Compressing Deep Neural Networks with Pruning, Trained Quantization and Huffman Coding. (2015). <https://arxiv.org/abs/1510.00149>
- [26] Song Han, Jeff Pool, John Tran, and William Dally. 2015. Learning both Weights and Connections for Efficient Neural Network. In *Advances in Neural Information Processing Systems*, C. Cortes, N. Lawrence, D. Lee, M. Sugiyama, and R. Garnett (Eds.), Vol. 28. Curran Associates, Inc. <https://proceedings.neurips.cc/paper/2015/file/ae0eb3eed39d2bcecf4622b2499a05fe6-Paper.pdf>
- [27] Kaiming He, Xiangyu Zhang, Shaoqing Ren, and Jian Sun. 2016. Deep Residual Learning for Image Recognition. In *Proceedings of the IEEE Conference on Computer Vision and Pattern Recognition (CVPR)*.
- [28] IBM. 2021. HELayers SDK with a Python API for x86. <https://hub.docker.com/r/ibmcom/helayers-pylab>
- [29] Nandan Kumar Jha, Zahra Ghodsi, Siddharth Garg, and Brandon Reagen. 2021. DeepReDuce: ReLU Reduction for Fast Private Inference. In *Proceedings of the 38th International Conference on Machine Learning (Proceedings of Machine Learning Research, Vol. 139)*, Marina Meila and Tong Zhang (Eds.). PMLR, 4839–4849. <https://proceedings.mlr.press/v139/jha21a.html>
- [30] Xiaoqian Jiang, Miran Kim, Kristin Lauter, and Yongsoo Song. 2018. Secure Outsourced Matrix Computation and Application to Neural Networks. In *Proceedings of the 2018 ACM SIGSAC Conference on Computer and Communications Security (Toronto, Canada) (CCS '18)*. New York, NY, USA, 1209–1222. <https://doi.org/10.1145/3243734.3243837>
- [31] Chirag Juvekar, Vinod Vaikuntanathan, and Anantha Chandrakasan. 2018. GAZELLE: A Low Latency Framework for Secure Neural Network Inference. In *27th USENIX Security Symposium (USENIX Security 18)*. USENIX Association, Baltimore, MD, 1651–1669. <https://www.usenix.org/conference/usenixsecurity18/presentation/juvekar>
- [32] Alex Krizhevsky, Ilya Sutskever, and Geoffrey Hinton. 2012. ImageNet Classification with Deep Convolutional Neural Networks. *Neural Information Processing Systems* 25 (01 2012). <https://doi.org/10.1145/3065386>
- [33] Yann LeCun, Corinna Cortes, and Christopher JC Burges. 1998. The MNIST database of handwritten digits. 10 (1998), 34. <http://yann.lecun.com/exdb/mnist/>
- [34] Ryan Lehmkuhl, Pratyush Mishra, Akshayaram Srinivasan, and Raluca Ada Popa. 2021. Muse: Secure Inference Resilient to Malicious Clients. In *30th USENIX Security Symposium (USENIX Security 21)*. USENIX Association, 2201–2218. <https://www.usenix.org/conference/usenixsecurity21/presentation/lehmkuhl>
- [35] Jian Liu, Mika Juuti, Yao Lu, and N Asokan. 2017. Oblivious Neural Network Predictions via MiniONN Transformations. In *Proceedings of the 2017 ACM SIGSAC Conference on Computer and Communications Security (CCS '17)*. Association for Computing Machinery, New York, NY, USA, 619–631. <https://doi.org/10.1145/3133956.3134056>
- [36] Qian Lou, Song Bian, and Lei Jiang. 2020. AutoPrivacy: Automated Layer-wise Parameter Selection for Secure Neural Network Inference. In *Advances in Neural Information Processing Systems*, H. Larochelle, M. Ranzato, R. Hadsell, M.F. Balcan, and H. Lin (Eds.), Vol. 33. Curran Associates, Inc., 8638–8647. <https://proceedings.neurips.cc/paper/2020/file/6244b2ba957c48bc64582cf2bcec3d04-Paper.pdf>
- [37] Qian Lou and Lei Jiang. 2021. HEMET: A Homomorphic-Encryption-Friendly Privacy-Preserving Mobile Neural Network Architecture. In *Proceedings of the 38th International Conference on Machine Learning (Proceedings of Machine Learning Research, Vol. 139)*, Marina Meila and Tong Zhang (Eds.). PMLR, 7102–7110. <https://proceedings.mlr.press/v139/lou21a.html>
- [38] Jian-Hao Luo, Jianxin Wu, and Weiyou Lin. 2017. ThiNet: A Filter Level Pruning Method for Deep Neural Network Compression. In *Proceedings of the IEEE International Conference on Computer Vision (ICCV)*.
- [39] Pratyush Mishra, Ryan Lehmkuhl, Akshayaram Srinivasan, Wenting Zheng, and Raluca Ada Popa. 2020. Delphi: A Cryptographic Inference Service for Neural Networks. In *29th USENIX Security Symposium (USENIX Security 20)*. USENIX Association, 2505–2522. <https://doi.org/10.1145/3411501.3419418>
- [40] Payman Mohassel and Peter Rindal. 2018. ABY3: A Mixed Protocol Framework for Machine Learning. In *Proceedings of the 2018 ACM SIGSAC Conference on Computer and Communications Security (CCS '18)*. Association for Computing Machinery, New York, NY, USA, 35–52. <https://doi.org/10.1145/3243734.3243760>
- [41] Payman Mohassel and Yupeng Zhang. 2017. SecureML: A System for Scalable Privacy-Preserving Machine Learning. In *2017 IEEE Symposium on Security and Privacy (SP)*, 19–38. <https://doi.org/10.1109/SP.2017.12>
- [42] Pavlo Molchanov, Stephen Tyree, Tero Karras, Timo Aila, and Jan Kautz. 2016. Pruning Convolutional Neural Networks for Resource Efficient Transfer Learning. (2016). <http://arxiv.org/abs/1611.06440>
- [43] Pascal Paillier. 1999. Public-Key Cryptosystems Based on Composite Degree Residuosity Classes. In *Advances in Cryptology - EUROCRYPT '99*, Jacques Stern (Ed.). Springer Berlin Heidelberg, Berlin, Heidelberg, 223–238. https://doi.org/10.1007/3-540-48910-X_16
- [44] Deevashwer Rathee, Mayank Rathee, Nishant Kumar, Nishanth Chandran, Divya Gupta, Aseem Rastogi, and Rahul Sharma. 2020. CryptFlow2: Practical 2-Party Secure Inference. In *Proceedings of the 2020 ACM SIGSAC Conference on Computer and Communications Security*. Association for Computing Machinery, New York, NY, USA, 325–342. <https://doi.org/10.1145/3372297.3417274>
- [45] M. Sadegh Riazi, Mohammad Samragh, Hao Chen, Kim Laine, Kristin Lauter, and Farinaz Koushanfar. 2019. XONN: XNOR-based Oblivious Deep Neural Network Inference. In *28th USENIX Security Symposium (USENIX Security 19)*. USENIX Association, Santa Clara, CA, 1501–1518. <https://www.usenix.org/conference/usenixsecurity19/presentation/riazi>
- [46] M Sadegh Riazi, Christian Weinert, Oleksandr Tkachenko, Ebrahim M Songhori, Thomas Schneider, and Farinaz Koushanfar. 2018. Chameleon: A Hybrid Secure Computation Framework for Machine Learning Applications. In *Proceedings of the 2018 on Asia Conference on Computer and Communications Security (ASIACCS '18)*. Association for Computing Machinery, New York, NY, USA, 707–721. <https://doi.org/10.1145/3196494.3196522> arXiv:1801.03239
- [47] Bitu Darvish Rouhani, M Sadegh Riazi, and Farinaz Koushanfar. 2018. DeepSecure: Scalable Provably-Secure Deep Learning. In *Proceedings of the 55th Annual Design Automation Conference (DAC '18)*. Association for Computing Machinery, New York, NY, USA. <https://doi.org/10.1145/3195970.3196023>
- [48] Jianbo Shi and Jitendra Malik. 2000. Normalized cuts and image segmentation. *IEEE Transactions on pattern analysis and machine intelligence* 22, 8 (2000), 888–905.
- [49] Sijun Tan, Brian Knott, Yuan Tian, and David J Wu. 2021. CryptGPU: Fast Privacy-Preserving Machine Learning on the GPU. In *2021 IEEE Symposium on Security and Privacy (SP)*, Vol. 2021-May. IEEE, 1021–1038. <https://doi.org/10.1109/SP40001.2021.00098> arXiv:2104.10949
- [50] Sameer Wagh, Shruti Tople, Fabrice Benhamouda, Eyal Kushilevitz, Prateek Mittal, and Tal Rabin. 2021. Falcon: Honest-Majority Maliciously Secure Framework for Private Deep Learning. *Proceedings on Privacy Enhancing Technologies* 2021, 1 (2021), 188–208. <https://doi.org/10.2478/popets-2021-0011> arXiv:2004.02229
- [51] Jun Wang, Chao Jin, Souhail Meftah, and Khin Mi Mi Aung. 2021. Popcorn: Paillier Meets Compression For Efficient Oblivious Neural Network Inference. <https://doi.org/10.48550/ARXIV.2107.01786>
- [52] Yang Yang, Sanmukh R. Kuppannagari, Rajgopal Kannan, and Viktor K. Prasanna. 2022. FPGA Accelerator for Homomorphic Encrypted Sparse Convolutional Neural Network Inference. In *2022 IEEE 30th Annual International Symposium on Field-Programmable Custom Computing Machines (FCCM)*, 1–9. <https://doi.org/10.1109/FCCM53951.2022.9786115>